

Automatic Task Parallelization of Dataflow Graphs in ML/DL models

Srinjoy Das

Univ. of Illinois at Urbana Champaign
Urbana-Champaign, USA
srinjoy3@illinois.edu

Lawrence Rauchwerger

Univ. of Illinois at Urbana Champaign
Urbana-Champaign, USA
rwerger@uiuc.edu

Abstract—Several methods exist today to accelerate Machine Learning(ML) or Deep-Learning(DL) model performance for training and inference. However, modern techniques that rely on various graph and operator parallelism methodologies rely on search space optimizations which are costly in terms of power and hardware usage. Especially in the case of inference, when the batch size is 1 and execution is on CPUs or for power-constrained edge devices, current techniques can become costly, complicated or inapplicable. To ameliorate this, we present a Critical-Path-based Linear Clustering approach to exploit inherent parallel paths in ML dataflow graphs. Our task parallelization approach further optimizes the structure of graphs via cloning and prunes them via constant propagation and dead-code elimination. Contrary to other work, we generate readable and executable parallel Pytorch+Python code from input ML models in ONNX format via a new tool that we have built called Ramiel. This allows us to benefit from other downstream acceleration techniques like intra-op parallelism and potentially pipeline parallelism. Our preliminary results on several ML graphs demonstrate up to $1.9\times$ speedup over serial execution and outperform some of the current mechanisms in both compile and runtimes. Lastly, our methods are lightweight and fast enough so that they can be used effectively for power and resource-constrained devices, while still enabling downstream optimizations.

Index Terms—Machine/Deep Learning, ML models, Dataflow Graphs, Parallelization, Clustering, Pytorch, ONNX.

I. INTRODUCTION

Deep Learning models have grown in size over the years and training or deploying them efficiently is of primary concern. Some of the well-known techniques to optimize these models involve fusion of operators [1] while others explore techniques like TASO [2] to automatically exploit various common algebraic transformations. As models and hardware have grown larger, the field has also moved towards improving methods to distribute models and huge training datasets across distributed systems through data, operator and pipeline parallelism also called 3D-parallelism [3]. The power and hardware resources required to train these models are enormous while search space-based methods that are usually employed to find good solutions for such device placement and distribution of compute/data require large amounts of time to obtain best-case answers.

However, for inference with a batch size of 1, which is a frequent use case, many of the standard techniques employed today [4], [5] that involve model/data/pipeline parallelism are inapplicable. There is no opportunity to perform parallel

pipelining because only a single pipeline is executed. Opportunities for data parallelism are also completely limited if the inference is for a single datapoint. In contrast to training which requires the entire model to be run repeatedly, and backpropagate weights, a single inference run executes just once and hence the time for compiling and preparing in any auto-tuning compilers becomes important. For example, the automated ML graph optimization framework Alpa [4] adds a 40 min compilation time overhead for optimizing training paths which should be avoided for inference. In this paper, we try to optimize the runtime of dataflow graphs used in inference for a batch size of 1 using fast automatic task-parallel algorithms. Our approach is to find structural/task-based parallelism in these graphs via clustering such that the makespan/scheduling time of these clusters is minimized, using fast algorithms.

Fig. 1 shows a snippet of the dataflow graph from Squeezenet. The dataflow graph of this model shows the presence of two mutually independent paths which converge and diverge several times. We task-parallelize such graphs using path-based clustering. We can create two clusters one for each path with the cross-cluster tensor dependences being evident as messages passing across the clusters. The clusters are then scheduled on CPU-multicores and run in parallel. An important feature of our approach is that we generate parallelized high-level runnable and readable Pytorch+Python code as opposed to most of today’s auto-tuning compilers for such systems. The reason being such an approach allows further downstream optimizations like intra-operator parallelism and pipeline parallelism to be applicable transparently. Our solution, though targeted for inference, may also be used as an initial optimization pass for training setups with high batch sizes. Since the goal of this work is to implement fast static compile time algorithms instead of costly search space-based methods with comparable performance profiles we resort to linear clustering algorithms. Finally, our method aims to augment the existing ML/DL dataflow graph parallelization strategies at the same time providing unique solution to the inference with batch size of 1 scenario.

A. The Contributions of this Work

- Implement a recursive critical-path-based Linear Clustering algorithm augmented with a new **cluster merging**

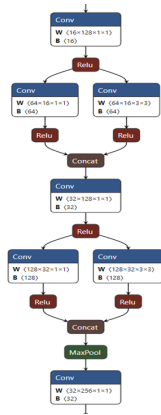


Fig. 1. Snippet of dataflow graph of SqueezeNet, showing the Convolution, Relu and Concat operations along with the tensor dependencies.

step. Additionally show how to prune/optimize such graphs using task cloning and constant propagation/dead-code elimination.

- Design and implement a new **Hyperclustering** algorithm that tries to exploit the slack times of such clusters, for batch size > 1 .
- A new tool called **Ramiel** that ingests ONNX [6] models and generates **runnable** Pytorch+Python methods that can be called from Python modules - each such method representing a parallel cluster of the dataflow graph. The generated code is easily debuggable, extendable and visually readable not precluding other standard downstream optimizations.

II. BACKGROUND

A key challenge for ML is determining how to split a large model across multiple heterogeneous devices to achieve the fastest possible training/inference speed. Today this is typically left to human experts, but determining an optimal device placement can be very challenging, particularly as neural networks grow in complexity or approach device memory limits.

Intra-Operator (called intra-op in literature) [4] parallelism is a method where a single ML/DL operation can be split up into several smaller operations of sub-elements in the tensor, and can be executed on multiple hardware resources- in a data-parallel fashion. Another approach called **Model Parallelism** [7] is used to break up the model into parts and distribute them on the parallel hardware. A common form of model parallelism is **Pipeline Parallelism** [8] where independent data samples are overlapped such that while one group of tasks execute on one set of data, another group of operations execute on a different set creating a pipeline similar to what we see in processor execution. **Data Parallelism** is also popular, especially for training, where batches of training samples are sub-divided into parallel mini-batches and executed on multiple hardware resources.

While many of these parallelism exploitation has been done by human experts, recent developments involve auto-parallel algorithms using search-space-based or dynamic-programming-based techniques. Some of the specific efforts that are of interest include the following. **Ding et al., 2021:** IOS: In Inter-Operator Scheduler for CNN Acceleration [9] the authors extensively study the parallelism between operators and propose Inter-Operator Scheduler (IOS) to automatically schedule multiple operators' parallel execution through a dynamic programming algorithm. **Wang et al., 2020:** In [10] the authors propose using *asynchronous scheduling* for task parallelism and hyper-tuning framework parameters (like the number of cores used) via a careful study of the models. **Yi et al., 2020:** Propose FastT [11], a module to work with the TensorFlow framework for automatically identifying and speeding up training over multiple GPUs inspired by DAG scheduling. **Zheng et al., 2022:** Alpa is an automated model-parallel training system that generates an execution plan unifying data, operator, and pipeline parallelism [4]. Its inter-op compilation pass distributes JAX IR into several stages, and slices the device cluster into a number of device meshes. Alpa's mechanism is costly as it involves solving integer or dynamic programming formulations and mainly targets GPU training. They beat manually tuned systems like Megatron [12] and Deepspeed [13]. **Zeng et al., 2022:** Use dynamic critical-path-based method called FD-DPS for speeding up model training, implementing intra-operator parallelism via graph search space exploration [14]. **Mirhoseini et al., 2017:** Propose an RNN-trained policy [5] which aims to optimize the device placement of models, but is very demanding in terms of computational power, energy costs and time.

III. METHODOLOGY

A. Observations on Structures of ML Graphs

1) *Potential Parallelism and Observations for ML graphs:* We study several ML models - SqueezeNet, GoogLeNet, Inception V3/V4, Yolo, BERT, RetinaNet and NASNet to implement our techniques. Some of these models exhibit fork-join kind of parallel structures - for example in SqueezeNet and GoogLeNet, while the graphs exhibit more complex structures in models like Yolo, BERT, RetinaNet and NASNet. Even for fork-join graph structures the out-degree or fan-out for such fork points may vary from one region of the graph to another. We define the potential *Parallelism* factor, a theoretical approximation of the parallelism that can be extracted from a dataflow graph. This factor is obtained by dividing the total amount of computation in a graph by the weighted length of the critical path (CP). More formally,

$$Parallelism = Wt.CostofNodes / Wt.CostofCriticalPath$$

where the *Wt.CostofNodes* signifies an approximation for the total computation and this is calculated by applying certain static weights to the operations, heavy DL operations like *Conv*, *Matmul* etc. having higher cost than simpler ones. Also a *Conv* using a bigger kernel of size 7×7 or 5×5 is assigned a higher cost compared to those of size 3×3

or 1×1 . Elementwise operations like *Relu* are assigned a cost of 1. Similarly *Wt.CostofCriticalPath* is calculated by considering the operations lying on the critical path of the graph. We also add a unit cost for each graph edge when computing the CP signifying some amount of overhead for the tensor dependences. It is due to this that for smaller graphs with long dependency chains, the potential parallelism may turn out to be < 1 .

Looking at Inception V3/V4 as shown in Fig. 2 we see that some parallel paths have very low computational intensity - implying that if these paths are scheduled on independent CPU cores, those cores may be idle most of the time. This observation leads to some strategies for parallelism exploitation that we have used, like task cloning and hyperclustering.

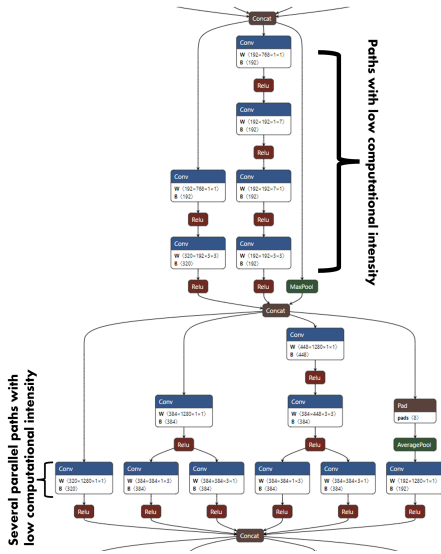


Fig. 2. Inception V3/V4 dataflow graph with paths/regions having low computational complexity that may reduce the parallelism exploitation opportunity.

BERT on the other hand (shown in Fig. 3) demonstrates a more complex graph structure where a bunch of nodes corresponding to the multi-headed attention (MHA) sequence [15], hang off one node - this structure being repeated many times, depending on the size of the Transformer module. The MHA sub-graph structure lends itself to further optimizations and simplification via constant propagation and dead-code elimination. We see similar opportunities for graph pruning in Yolo V5 also.

One of the biggest and most complex models we have handled is NASNet. NASNet belongs to the family of Neural Architectural Search models [16] and its dataflow graph contains more than a thousand nodes and edges. It has a huge fan-out at certain parts due to the search nature of the model. The graph is a mix of computationally heavy Conv2D nodes and simpler operations like slice, gather and reshape. There is abundant parallelism throughout the graph which leads to high speedup potential. A part of the structure is shown in Fig. 4. NASNet also lends itself to substantial graph pruning.

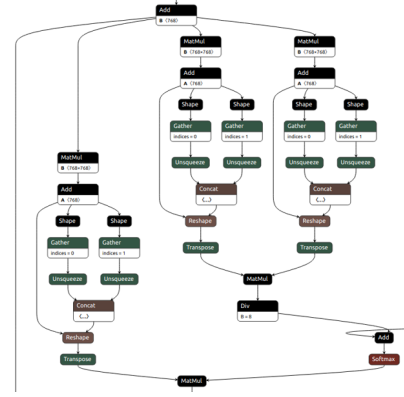


Fig. 3. BERT: This is a dataflow graph from one of the popular Transformer models, where we see that a certain kind of structure that arises repeatedly due to the Multi-Headed Attention mechanism that is the central premise of the model.

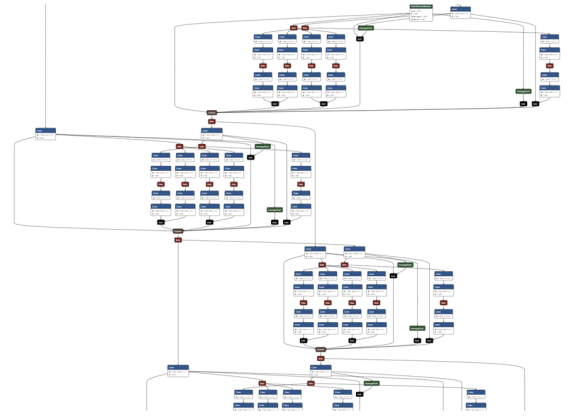


Fig. 4. NASNet: A neural architectural search model whose dataflow graph is big and exhibits abundant parallelism.

TABLE I
POTENTIAL PARALLELISM THAT EXISTS IN ML DATAFLOW GRAPHS.

Model Name	#Nodes	Wt. NodeCost	Wt. CP	\parallel_{ism}
Squeezenet	66	187	218	0.86×
Googlenet	153	373	264	1.4×
Inception V3	238	1136	829	1.37×
Inception V4	339	1763	1334	1.32×
Yolo V5	280	730	619	1.18×
Retinanet	450	1291	1102	1.2×
BERT	963	21357	16870	1.27×
NASNet	1426	8147	2187	3.7×

2) *Some dataflow graph metrics:* Table I represents some metrics of the dataflow graphs. We observe that some of the dataflow graphs exhibit a limited amount of parallelism. For example, in Squeezenet, the potential speedup is 0.86× which may likely cause slowdown when run on hardware. Inception V3/V4 etc. on the other hand demonstrate parallelism potential of around 1.3× to 1.4×. Finally there are models like NASNet

that exhibit potential parallelism of the order of $3.7\times$. We would like to use this static parallelism metric as an indicator of actual speedup on hardware when we parallelize the models.

B. Task Parallelization via Linear Clustering (LC)

Clustering and scheduling a dataflow graph involves splitting the graph into a set of nodes, where each set would be a target for a different piece of hardware viz. a core of a CPU. Given a task graph, the **clustering** problem can be defined as the process of mapping the nodes of graphs onto labelled clusters C_0, C_1, \dots, C_k such that the running time of the parallel code is minimized. All the tasks that belong to the same cluster execute on the same core while the clusters themselves are run on separate cores communicating via messages.

The Recursive Critical-Path-based Linear Clustering(LC) technique by Kim et al. [17] was chosen as the clustering algorithm. It involves finding a critical path at the outset. Once a critical path is found, its nodes are removed from contention, and a new iteration begins to find the next critical path through the remainder graph. These iterations continue until there are no more paths available. What we obtain is a clustering of the graph where each cluster is the longest path obtainable at that instance of the graph and is linear in nature. The passes in our LC algorithm are the following: i) Graph creation pass - Converts an input ONNX model into an internal representation ii) Distance pass - Computes the weighted distance of each node from the end node of the graph and stores in *distance_to_end* iii) Critical path-based clustering pass and iv) Cluster merging pass. Details on last two passes follow.

1) *Critical Path-Based Clustering pass*: We use the critical path algorithm recursively to linearly cluster the entire graph. Algorithm 1 contains the details. Fig. 5 shows how the clusters look when LC is applied to Squeezenet’s dataflow graph. While the main cluster C_1 running on one core consists of heavier **Conv2D**→**Relu**→**Concat** ops pattern repeated multiple times, the side clusters C_2, C_3 and C_4 are just small clusters consisting of lighter **Conv2D**→**Relu** ops pattern. To avoid multiple small clusters we apply a cluster merging pass post-LC, to merge **non-overlapping clusters**. An example of how the clusters look after clustering (a) before merging and (b) after merging is given in Fig. 5.

2) *Cluster Merging pass*: Linear clustering has some drawbacks when applied to the ML dataflow graphs. Due to the nature of these graphs, zeroing out the nodes in the critical path leaves behind a disconnected graph in several cases. Also, the paths generated become shorter than the previous paths because disjointedness prevents them from fully extending. The cluster merging algorithm (Algorithm 2 and 3) remedies this by iteratively combining clusters that do not overlap with respect to their start/end times and is computationally linear in the number of clusters already created. Algorithm 2 is called iteratively in Algorithm 3 till a fixed point is reached and no further merging is possible. Table II shows the number of clusters created by the original Linear Clustering pass

Input : Dataflow Graph - *Graph*

Output: A clustering of the nodes of Graph, C_1, \dots, C_k , s.t.
 $C_i \cap C_j == \phi$ and every node appears in some C_i

```

nodes ← Graph.nodes ;
outgoing_edges ← Outgoing edges of nodes ;
incoming_edges ← Incoming edges of nodes ;
allClusters ← { } ;
while nodes ≠ ϕ do
  # Start a new Critical Path ;
  readyL ← List of Nodes s.t. indegree of node is 0 ;
  cNode ← argmaxn(distance_to_end(n)), n ∈ readyL ;
  newCluster ← {cNode} ;
  nodes ← nodes - {cNode} ;
  while outgoing_edges(cNode) ≠ ϕ do
    succ ← successor nodes of cNode ;
    sNode ← argmaxn(distance_to_end(n)), n ∈ succ ;
    newCluster ← newCluster ∪ {sNode} ;
    nodes ← nodes - {sNode} ;
    Remove all outgoing_edges(cNode) other than
      cNode → sNode from outgoing_edges;
    Remove all incoming_edges(sNode) from
      incoming_edges;
    cNode ← sNode ;
  end
  # newCluster contains the Critical Path ;
  allClusters ← allClusters ∪ newCluster;
end
return allClusters;

```

Algorithm 1: Recursive Linear Clustering

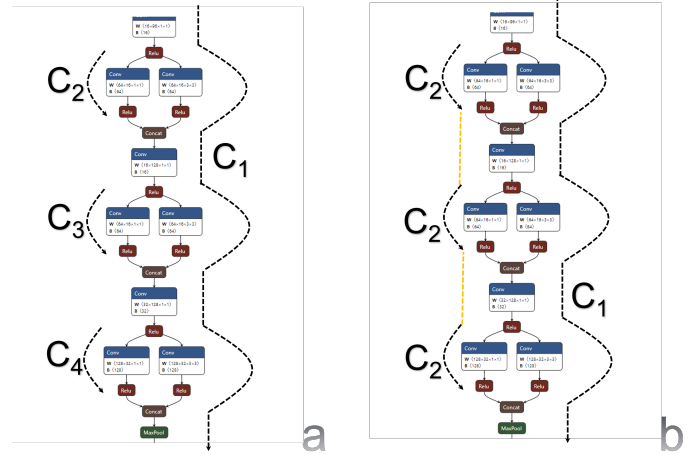


Fig. 5. a. Shows the clusters C_1, \dots, C_4 . b. Several side clusters C_2, C_3 and C_4 are merged to form a single cluster C_2 .

compared to the number of clusters finally produced by the cluster merging pass. For several models the number of linear clusters decreases significantly thereby helping to manage the parallel code generation and subsequent overheads.

C. Dataflow Graph Pruning via Constant Propagation (CP) and Dead-Code Elimination (DCE)

Constant propagation and folding eliminate constants that are used as part of the model. Further, Dead Code elimination

Input : Clusters - C_1, \dots, C_k
Output: a. The merged clusters $MC_1, \dots, MC_m, m \leq k$,
b. Boolean flag mergeDone

MergedClusters $\leftarrow \{\}$; skipCluster $\leftarrow \{\}$;
mergeDone \leftarrow False ;
foreach cluster cl_1 **in** clusters **do**
 foreach cluster cl_2 **in** clusters **do**
 if $cl_1 \neq cl_2 \wedge (cl_1 \text{ and } cl_2 \notin \text{skipCluster})$ **then**
 sSpan of a cluster \leftarrow
 distance_to_end(entry_node(cluster)) ;
 eSpan of a cluster \leftarrow
 distance_to_end(exit_node(cluster)) ;
 # Check that cluster spans do not overlap ;
 if $sSpan(cl_1) < eSpan(cl_2) \parallel$
 $sSpan(cl_2) < eSpan(cl_1)$ **then**
 Create a merged cluster $MC_i = cl_1 \cup cl_2$;
 MergedClusters \leftarrow MergedClusters $\cup MC_i$
 ;
 # Do not process cl_1 and cl_2 further ;
 # So add them to skipCluster ;
 add cl_1 and cl_2 to skipCluster;
 mergeDone \leftarrow True ; break ;
 end
 end
 end
 # if cl_1 is not merged with any cluster ;
 # Add cl_1 as a standalone merged cluster ;
 if cl_1 not Merged **then**
 MergedClusters \leftarrow MergedClusters $\cup cl_1$;
 end
end
return MergedClusters, mergeDone ;

Algorithm 2: MergeClusters

Input : Clusters - C_1, \dots, C_k
Output: The final merged clusters $MC_1, \dots, MC_m, m \leq k$

nClus \leftarrow Clusters;
mergeDone \leftarrow True ;
while mergeDone == True **do**
 MergedClusters, mergeDone \leftarrow MergeClusters(nClus) ;
 nClus \leftarrow MergedClusters;
end
return MergedClusters ;

Algorithm 3: Iterative Cluster Merging

TABLE II
NUMBER OF CLUSTERS FORMED FOR THE ML GRAPHS, BEFORE AND AFTER **Cluster Merging**.

Model	Before Merging	After Merging
Squeezenet	9	2
Googlenet	30	4
Inception V3	38	6
Inception V4	55	6
Yolo V5	29	12
BERT	76	5
Retinanet	16	10
NASNet	244	67

can remove these operator nodes. We leverage ONNX Runtime (**onnxruntime**) [18] to perform this graph transformation. Viewing the simplified graph in Fig. 6(b) clearly shows how

the complexity and number of paths through just one section of the graph reduce from Fig. 6(a). If the Cluster Merging Pass is viewed as a **Vertical branch compression** strategy, then constant propagation is a **Horizontal branch reduction** strategy. A table comparing the number of parallel clusters generated by onnxruntime before and after the optimization on the graph is shown in Table III.

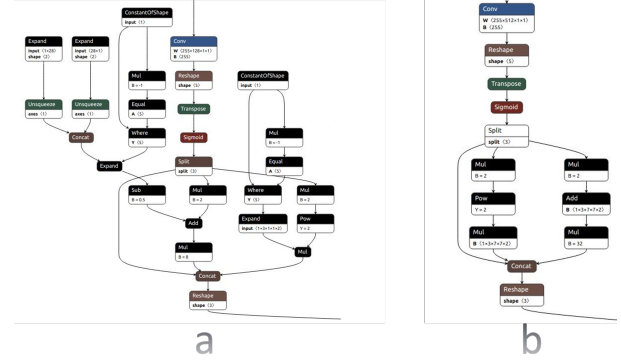


Fig. 6. Parts of Model Yolo before and after constant propagation.

TABLE III
CLUSTER SIZE POST CONSTANT PROPAGATION AND DEAD-CODE ELIMINATION.

Model Name	Before Const Prop	After Const Prop
YOLO V5	12	9
NASNet	67	9
BERT	5	3

D. Graph Cloning

Graph Cloning is a well-studied optimization in parallel computing whereby graph nodes are cloned or replicated across multiple processors or hardware so that the overall schedule time or latency of executing the graph is reduced [19]. Cloning is usually employed in distributed message-passing scenarios to overcome communication bottlenecks but we have applied it to our case and observed improved runtimes. Though cloning usually results in improved performance it comes at the price of *redundant* computation happening on multiple clusters. Also, cloning can blow up the size of the graph exponentially. Hence, it should be applied with care and in limited setting. Cloning in Inception V3 dataflow graph is shown in Fig. 7.

E. Hyperclustering: Beyond Linear Clustering

When we run some profiling on the parallel code that we generate it is seen that every time a cluster waits to receive data from another cluster there arises a slack or gap especially if the data is not ready in another cluster. This imbalance is a window of opportunity if inference is done with small batch sizes > 1 . Taking ideas from **hyperthreading** as applied to modern CPU cores, we have multiple inference samples in flight which is possible when the batch size for inference is

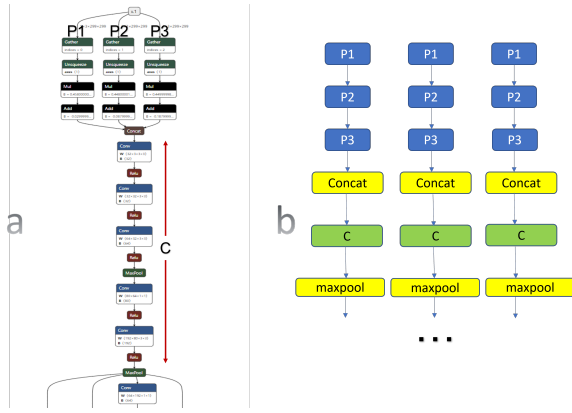


Fig. 7. Cloning in Inception V3.

greater than 1. This helps in reducing the slacks. Fig. 8 shows the hyperclusters created for a batch size of 2 for Squeezenet. This technique can be also applied for higher batch sizes which have the advantage of reducing and probably eliminating a large part of the slack.

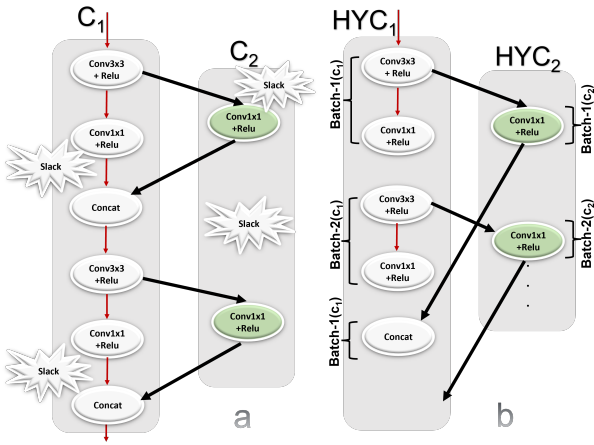


Fig. 8. The creation of hyperclusters is shown for Squeezenet. (a) shows the original clustering and b) shows the hyperclusters - HYC_1 and HYC_2 being created with copies from two images from a batch size of 2.

A more efficient method of creating hyperclusters is by aligning operations from multiple batches of dissimilar clusters so that better load balance is achieved. For each set of operations of batch_i, the next set of operations will be those of batch_j, but instead of picking operations from the same cluster, it uses the operations from one of the other clusters such that the clusters now have more balanced operational efficiency. This approach is outlined in Fig. 9 where for the same Squeezenet example, we switch the cluster operations while creating the new hyperclusters. It can be observed that compared to hyperclustering we now have a better load balanced cluster, as we have 5 operations in $SHYC_1$ and 3 operations in $SHYC_2$ versus 5 and 2 in HYC_1 and HYC_2 . We refer to such Hyperclusters as **Switched Hyperclusters**.

Implementing switched hyperclusters automatically is complex for more involved ML graphs. At present we handle this automatically for simple graphs like Squeezenet and manually for more complex graphs after observing the profile data.

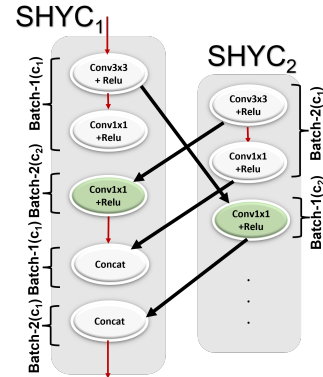


Fig. 9. Switched hypercluster for Squeezenet.

IV. IMPLEMENTATION DETAILS

For our e2e implementation we built a new tool called **Ramiel**. The high-level architecture of Ramiel is provided in Fig. 10. Ramiel’s inputs are ONNX models. These models are extracted from Pytorch 2.0 repository [20] and Huggingface [21] as well as ONNX model zoo [22]. ONNX provides a mechanism to load and read the frozen graph representations of the ML models via various APIs. Ingesting ONNX models for runnable Pytorch+Python code generation is non-trivial. Also, the conventions used in ONNX to represent the ML/DL ops are sometimes significantly different from their avatars in Pytorch. In this tool, the *Model2Graph* Converter stage is responsible for taking an ONNX graph and convert it to an internal in-memory graph format. onnxruntime may be used as a separate plugin at the input stage to perform constant propagation and dead code elimination and return an optimized ONNX model that is fed to this converter. An optional *Cloning* stage is used to do limited cloning of graphs if possible. Next, the *Clustering* stage is responsible for performing the linear clustering algorithm and cluster merging. When the batch size is > 1 , the *Hyperclustering* stage is triggered and the operations in different clusters are interleaved. Finally, *ParallelCodegenerator* is responsible for converting the graph into its corresponding PyTorch+Python code. When profiling is enabled a profile database holds information about the execution trace and the slacks during communication which can be used offline.

Since our system is built on Python and Pytorch, we step away from threads due to the limitations of the Global Interpreter Lock [23] and use Python processes. Algorithm 4 provides an overview of the parallel code generation logic. The inputs to the parallel code generation pass are the merged clusters. Each cluster/path gets its own function, where such functions are finally forked by Python processes.

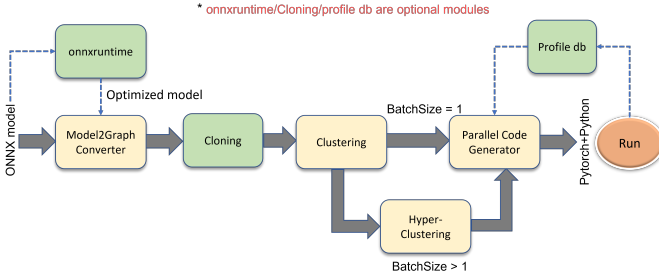


Fig. 10. Architecture of **Ramiel**.

Input : Clusters – $C_1 \dots C_m$

Output: Pytorch + Python code for each cluster C_i , encapsulated as a method

```

foreach cluster  $C_i$  do
  Generate cluster  $C_i$ 's Python method definition and
  signature with name and input/output tensors;
  foreach node  $n$  in  $C_i$  do
    foreach each successor node  $succn$  do
      if  $succn$  belongs to a remote cluster  $C_j$  then
        | Generate a send message using queue.put();
      end
    end
    foreach predecessor node  $predn$  do
      if  $predn$  belongs to a remote cluster  $C_j$  then
        | Generate a recv message using queue.get();
      end
    end
    Generate a new SSA-name for the output variable of
    the node  $n$  called outVar;
    GeneratePytorchCodeForOperandType( $n$ );
  end
end

```

Algorithm 4: Parallel Code Generation

Our algorithm also generates all the synchronizing **get/put** primitives using the message passing bi-directional queues. **GeneratePytorchCodeForOperandType** is a method which calls the equivalent Pytorch operator. A snippet of a 2-cluster parallel code of Squeezenet is provided in Fig. 11. To ensure completeness and to evaluate the parallel code generation, a single core non-parallel version of the code is also generated by Ramiel.

V. EXPERIMENTAL RESULTS

Our implementation is written in Python 3.8 and Pytorch is used as the ML framework. The parallel code that is generated by the tool Ramiel also targets PyTorch and Python 3.8. An Intel 12-core 24-thread 1.1Ghz Xeon Gold machine was used for all runtime experiments. **Other than what is specified for hyperclustering experiments, all other experiments have been conducted with a batch size of 1.** The experiments target ML dataflow graphs for inference setups.

A. Performance of Linear Clustering (LC)

Our first set of experiments shown in Table IV are execution time comparisons between sequential and parallel code generated by the Linear Clustering (LC) algorithm after cluster

merging. This does not take into account further optimizations such as constant propagation, cloning or hyperclustering. Both the sequential and parallel code are automatically generated by Ramiel. The results in this table signify a direct correlation to the potential parallelism factor. Squeezenet demonstrates a parallelism factor of 0.86, a value lower than 1 indicating that it is infeasible to attempt to parallelize this. When the parallelism factor rises higher than 1 there is a clear trend of speedup in runtime. NASNet shows the highest speedup of $1.7\times$ for LC though the potential parallelism stands much higher at $3.7\times$. This is likely due to the large number of clusters (67 of them) created by LC and the potential overhead of scheduling and running them on Pytorch. However, with advanced optimizations the number of clusters decreases substantially pushing this performance higher. For other graphs like Inception V3/V4 the achieved parallelism is close to the projected values. Yolo and BERT have low projected parallelism. Hence we achieve a slight drop in performance with LC for Yolo and only a moderate $1.07\times$ with BERT. Retinanet beats the static parallelism estimate by achieving $1.3\times$ speedup.

B. Performance of LC + Downstream Intra-Op Parallelism

We enable Intra-op parallelism as a downstream optimization post-LC, as shown in Table V and we compare our LC+Intra-op runtimes with pure intra-op runtimes instead of comparing with sequential runs. In Pytorch, the operations are parallelized (intra-op parallelism) using OpenMP [24] constructs provided by Pytorch. Hence, by changing the number of OpenMP threads used, we can vary the degree of intra-op parallelism. We enable OpenMP threads in Pytorch using the Intel OpenMP library (libiomp) [25]. Enabling intra-op parallelism allows operations such as a single convolution to use multiple threads. We show that using a combination of LC + downstream intra-op parallelism helps get better speedup than pure intra-op parallelism or LC in most of the cases. Some of the models demonstrate slight slowdowns or plateauing with higher openmp threads, which is due to oversubscription of the CPU cores.

C. Performance of LC + Constant Propagation(CP) + Dead-code Elimination(DCE)

When Constant Propagation and Dead Code Elimination are applied via **onnxruntime** as shown in Table VI (here S_{LC} and S_{LC+DCE} stand for respective speedups), we see gains for those graphs where constant propagation prunes the graphs. Squeezenet, Googlenet and Inception models do not demonstrate the presence of constants. However, Yolo, NASNet and BERT present several opportunities to carry out dead-code elimination. Yolo had an apparent slowdown with a 4% loss in performance with LC when not using constant propagation and subsequently shows a performance improvement with a close to 10% upswing in speedup. NASNet also gains well with an $1.9\times$ uplift when compared to $1.7\times$ without CP and DCE. Overall, CP+DCE seems to be an essential optimization

```

def fparcluster_1(x: torch.Tensor) -> torch.Tensor:
    x1_0 = nn.Conv2d(3,96,kernel_size=7, padding=0, stride=2)(x)
    x1_1 = nn.ReLU(inplace=True)(x1_0)
    x1_2 = nn.MaxPool2d(kernel_size=3, padding=0, stride=2)(x1_1)
    x1_3 = nn.Conv2d(96,16,kernel_size=1, padding=0, stride=1)(x1_2)
    x1_4 = nn.ReLU(inplace=True)(x1_3)
    qu1_2.put(x1_4.numpy())

    x1_5 = nn.Conv2d(16,64,kernel_size=3, padding=0, stride=1)(x1_4)
    x1_6 = nn.ReLU(inplace=True)(x1_5)

    x_2 = torch.from_numpy(qu1_2.get(block=True))
    x1_7 = torch.cat([x1_6,x_2], 1)
    x1_8 = nn.Conv2d(128,16,kernel_size=1, padding=0, stride=1)(x1_7)
    x1_9 = nn.ReLU(inplace=True)(x1_8)
    qu1_2.put(x1_9.numpy())

    x1_10 = nn.Conv2d(16,64,kernel_size=3, padding=0, stride=1)(x1_9)
    x1_11 = nn.ReLU(inplace=True)(x1_10)

    x_2 = torch.from_numpy(qu2_1.get(block=True))
    x1_12 = torch.cat([x1_11,x_2], 1)
    x1_13 = nn.Conv2d(128,32,kernel_size=1, padding=0, stride=1)(x1_12)
    x1_14 = nn.ReLU(inplace=True)(x1_13)
    qu1_2.put(x1_14.numpy())
    ...

def fparcluster_2(x: torch.Tensor) -> torch.Tensor:
    x_1 = torch.from_numpy(qu1_2.get(block=True))
    x2_0 = nn.Conv2d(16,64,kernel_size=1, padding=1, stride=1)(x_1)
    x2_1 = nn.ReLU(inplace=True)(x2_0)
    qu2_1.put(x2_1.numpy())
    x_1 = torch.from_numpy(qu1_2.get(block=True))

    x2_2 = nn.Conv2d(16,64,kernel_size=1, padding=1, stride=1)(x_1)
    x2_3 = nn.ReLU(inplace=True)(x2_2)
    qu2_1.put(x2_3.numpy())
    x_1 = torch.from_numpy(qu1_2.get(block=True))

    x2_4 = nn.Conv2d(32,128,kernel_size=1, padding=1, stride=1)(x_1)
    x2_5 = nn.ReLU(inplace=True)(x2_4)
    qu2_1.put(x2_5.numpy())
    x_1 = torch.from_numpy(qu1_2.get(block=True))
    ...

```

Fig. 11. Snippet of Parallel Code Generated for Clusters of Squeezenet using Pytorch+Python. The inter-cluster communication primitives are highlighted.

TABLE IV
PERFORMANCE OF LINEAR CLUSTERING (LC) ALGORITHM.

Model Name	Parallelism	No. of clusters	Seq Time(ms)	Parallel Time(ms)	Speedup
Squeezenet	0.86×	2	85	103	0.83×
GoogleNet	1.4×	4	188	156	1.2×
Inception V3	1.37×	6	559	422	1.32×
Inception V4	1.32×	6	1212	840	1.44×
Yolo V5	1.18×	12	790	820	0.96×
BERT	1.27×	6	3296	3071	1.07×
Retinanet	1.2×	10	4311	3361	1.3×
NASNet	3.7×	67	2271	1351	1.7×

TABLE V
PERFORMANCE OF LINEAR CLUSTERING (LC) + DOWNSTREAM INTRA-OP PARALLELISM (* Both Par and Seq have intra-op enabled).

Model Name	NUM_THREADS=2			NUM_THREADS=4			Overall Speedup Best Overall = Best Seq Time/Best Par Time
	Par(ms)	Seq(ms)	Speedup	Par(ms)	Seq(ms)	Speedup	
Squeezenet	86	67	0.78×	87	58	0.67×	0.67×
Googlenet	143	163	1.14×	143	143	1.00×	1.00×
Inception V3	375	476	1.27×	357	438	1.23×	1.23×
Inception V4	676	983	1.45×	699	826	1.18×	1.22×
Retinanet	2100	2575	1.23×	1462	1633	1.12×	1.12×
NASNet	1297	1664	1.3×	-	-	-	1.3×

TABLE VI
PERFORMANCE OF LC WHEN AUGMENTED WITH CONSTANT PROPAGATION AND DEAD-CODE ELIMINATION.

Model	S_{LC}	S_{LC+DCE}
Yolo V5	0.96×	1.06×
BERT	1.07×	1.15×
NASNet	1.7×	1.91×

to prune ML/DL dataflow graphs for improved clustering and runtimes.

D. Performance of LC + Cloning

Restricted cloning has been applied in our work, mostly at the top half of the dataflow graphs to reduce the blow-up in terms of size. For our experiments, we have cloned the smaller dataflow graphs and avoided bigger graphs like NASNet. Cloning provides moderate boost in performance with up to 8% improvement. Details are in Fig. 12.

E. Overall Performance and Comparison with Inter-Operator Scheduler(IOS)

In Table VII we show the overall impact of LC, CP+DCE, and cloning when compared to sequential implementation. We also compare our inference speedup with the work done by

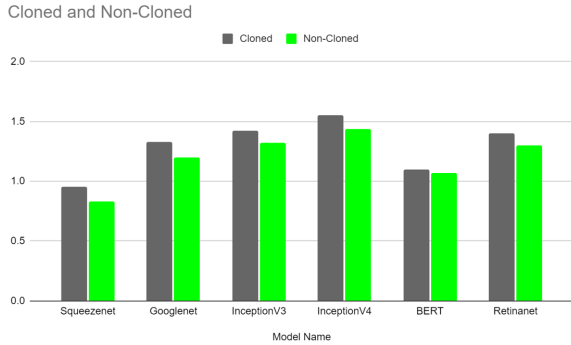


Fig. 12. Performance uplift of cloned models versus non-cloned models.

TABLE VII
PERFORMANCE OF LC WHEN AUGMENTED WITH CP+DCE+CLONING.

Model Name	S_{LC}	S_{LC+DCE}	$S_{LC+Cloning}$	$S_{Overall}$
Squeezenet	0.83 \times	-	0.95 \times	0.95 \times
GoogleNet	1.2 \times	-	1.33 \times	1.33 \times
Inception V3	1.32 \times	-	1.42 \times	1.42 \times
Inception V4	1.44 \times	-	1.55 \times	1.55 \times
BERT	1.07 \times	1.15 \times	1.1 \times	1.18 \times
Yolo V5	0.96 \times	1.06 \times	-	1.06 \times
Retinanet	1.3 \times	-	1.4 \times	1.4 \times
NASNet	1.7 \times	1.91 \times	-	1.91 \times

Ding et al. [9] named IOS. In IOS the authors extract inter-operator parallelism for small batch sizes using a dynamic-programming algorithm. Hence, this work is closest to ours as we also extract inter-operator/task parallelism for small batch sizes. Table VIII shows the comparison of speedup attained by our work ($Speedup_{Ours}$) compared to IOS - $Speedup_{IOS}$, for benchmarks that are in common between our experimental studies. These are Squeezenet, Inception and NASNet. CT(s) stands for compile-time in seconds. Our work (Table VIII) is much faster than IOS with respect to runtimes for NASNet (1.91 \times vs 1.4 \times), on par for Inception (1.6 \times) and moderately slower on Squeezenet (which is due to higher Python process overheads in our implementation). On the compile time front IOS is significantly costlier than our mechanism. Even for large graphs like NASNet/BERT/Yolo etc. we complete our code generation in a few seconds - NASNet consuming the highest time of 9.7 seconds. On the other hand, IOS takes about 90 minutes to generate the schedule for NASNet and around a minute each for Squeezenet and Inception. Hence, our mechanism is faster by 10 \times to 500 \times with similar to better runtimes, thereby saving on important parameters like power and cost.

F. Performance of Hyperclustering

For Hyperclustering, we use batch sizes of 2, 4, 8 and 12 and observe the relative speedup when compared to the sequential version of the codes. As evident from Fig. 13, the potential speedup exploitable when Hyperclustering is used are significant. The speedup rises as we increase the

TABLE VIII
PERFORMANCE COMPARISON OF OUR WORK WITH IOS.

Model Name	$Speedup_{Ours}$	CT(s)	$Speedup_{IOS}$	CT(s)
Squeezenet	0.95 \times	2.2s	1.15 \times	60s
Inception	1.55 \times	5.2s	1.59 \times	60s
NASNet	1.91 \times	9.7s	1.4 \times	5400s

number of threads (up to hardware thread limit). The switched Hyperclustering algorithm further improves performance when compared to the non-switched versions of the code with performance uplifts of around 30% in the best cases as evident in Fig. 14.

VI. CONCLUSION AND FUTURE WORK

Here we have studied the important problem of automatically task-parallelizing ML dataflow graphs where batch size is 1 or a small positive number. Our goal has been to create fast algorithms that perform well. We devise linear clustering-based mechanisms to extract task parallelism from models augmented by advanced compiler optimizations like cloning and DCE. Our tool, Ramiel, converts ONNX models into parallel Pytorch+Python and demonstrates the characteristics of readability, executability and extendability via further optimizations such as intra-op/model/pipeline parallelism. New strategies like hyperclustering may turn out to be beneficial in training setups too. Finally, comparison with recent literature demonstrates the competitiveness of our approach. We have demonstrated that we can achieve fast compile time while obtaining similar performance as evidenced in (Table VIII). Future work involves further experimentation in power and resource-constrained settings as well as devising more powerful optimizations for graph reductions, possibly via tools like MLIR.

REFERENCES

- [1] T. Chen, T. Moreau, Z. Jiang, H. Shen, E. Yan, L. Wang, Y. Hu, L. Ceze, C. Guestrin, and A. Krishnamurthy, "TVM: End-to-End Optimization Stack for Deep Learning," University of Washington, WA, Tech. Rep. UW-CSE-2017-12-01, Dec. 2017.
- [2] Z. Jia, O. Padon, J. Thomas, T. Warszawski, M. Zaharia, and A. Aiken, "TASO: Optimizing Deep Learning Computation with Automatic Generation of Graph Substitutions," in *SOSP '19: Proceedings of the 27th ACM Symposium on Operating Systems Principles*, Ontario, Canada, Oct. 2019, pp. 47–62.
- [3] J. Song, J. Yim, J. Jung, H. Jang, H. Kim, Y. Kim, and J. Lee. (2023, Jan.) Optimus-CC: Efficient Large NLP Model Training with 3D Parallelism Aware Communication Compression. [Online]. Available: <https://arxiv.org/pdf/2301.09830.pdf>
- [4] L. Zheng, Z. Li, H. Zhang, Y. Zhuang, Z. Chen, Y. Huang, Y. Wang, Y. Xu, D. Zhuo, E. P. Xing, J. E. Gonzalez, and I. Stoica, "Alpa: Automating Inter- and Intra-Operator Parallelism for Distributed Deep Learning," in *Proceedings of the 16th USENIX Symposium on Operating Systems Design and Implementation (OSDI 22)*, Carlsbad, CA, USA, Jul. 2022, pp. 559–578.
- [5] A. Mirhoseini, H. Pham, Q. V. Le, B. Steiner, R. Larsen, Y. Zhou, N. Kumar, M. Norouzi, S. Bengio, and J. Dean, "Device Placement Optimization with Reinforcement Learning," in *ICML'17: Proceedings of the 34th International Conference on Machine Learning*, Sydney, Australia, Aug. 2017, p. 2430–2439.
- [6] ONNX - Open Neural Network Exchange. [Online]. Available: <https://onnx.ai/>

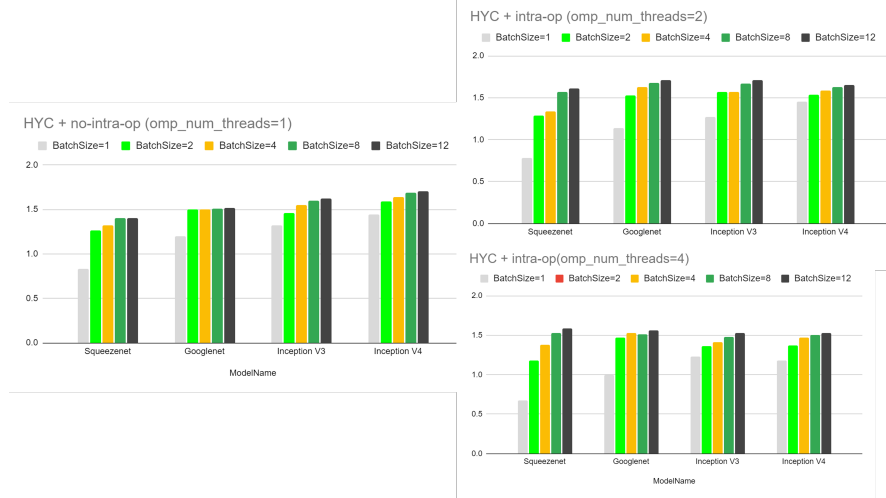


Fig. 13. Performance of Hyperclustering with batch sizes of 2, 4, 8, 12 with and without intra-op.

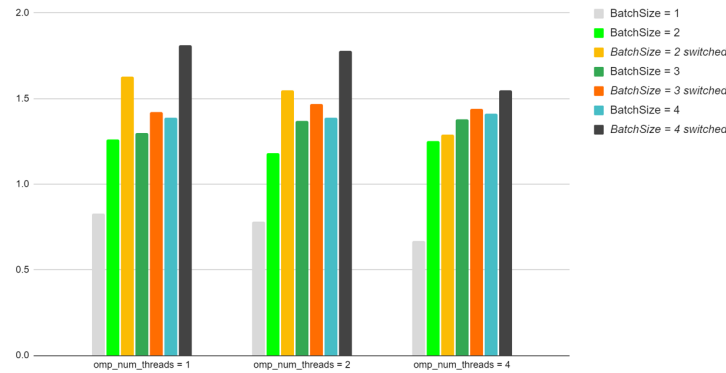


Fig. 14. Performance of Switched Hyperclustering with batch sizes of 2, 3, 4 with and without intra-op for Squeezenet

- [7] Introduction to Model Parallelism. [Online]. Available: <https://docs.aws.amazon.com/sagemaker/latest/dg/model-parallel-intro.html>
- [8] Y. Huang, Y. Cheng, A. Bapna, O. Firat, M. X. Chen, D. Chen, H. J. Lee, J. Ngiam, Q. V. Le, Y. Wu, and Z. Chen, "GPipe: Efficient Training of Giant Neural Networks using Pipeline Parallelism," in *NIPS'19: Proceedings of the 33rd International Conference on Neural Information Processing Systems*, Vancouver, Canada, Dec. 2019, pp. 103–112.
- [9] Y. Ding, L. Zhu, Z. Jia, G. Pekhimenko, and S. Han, "IOS: Inter-Operator Scheduler for CNN Acceleration," in *Proceedings of Machine Learning and Systems (MLSys)*, Virtual, Apr. 2021.
- [10] Y. E. Wang, C. J. Wu, X. Wang, K. Hazelwood, and D. Brooks, "Exploiting parallelism opportunities with deep learning frameworks," *ACM Transactions on Architecture and Code Optimization*, vol. 18, Issue 1, pp. 1–23, Dec. 2020.
- [11] X. Yi, Z. Luo, C. Meng, M. Wang, G. Long, C. Wu, J. Yang, and W. Lin, "Fast Training of Deep Learning Models over Multiple GPUs," in *Middleware '20: Proceedings of the 21st International Middleware Conference*, Sydney, Australia, Dec. 2020, p. 105–118.
- [12] Z. Cai, K. Ma, X. Yan, Y. Wu, Y. Huang, J. Cheng, T. Su, and F. Yu. (2020, Apr.) TensorOpt: Exploring the Tradeoffs in Distributed DNN Training with Auto-Parallelism. [Online]. Available: <https://arxiv.org/pdf/2004.10856.pdf>
- [13] S. Rajbhandari, J. Rasley, O. Ruwase, and Y. He, "ZeRO: Memory Optimizations Toward Training Trillion Parameter Models," in *SC '20: Proceedings of the International Conference for High Performance Computing, Networking, Storage and Analysis*, Virtual, Nov. 2020, pp. 1–16.
- [14] Y. Zeng, W. Wang, Y. Ding, J. Zhang, Y. Ren, and G. Yi, "Adaptive Distributed Parallel Training Method for a Deep Learning Model Based on Dynamic Critical Paths of DAG," *Mathematics, MDPI*, vol. 10(24), pp. 1–21, Dec. 2022.
- [15] J. Devlin, M. W. Chang, K. Lee, and K. Toutanova, "BERT: Pre-training of Deep Bidirectional Transformers for Language Understanding," in *Proceedings of NAACL-HLT*, Minneapolis, USA, Jun. 2019, pp. 4171–4186.
- [16] B. Zoph, V. Vasudevan, J. Shlens, and Q. V. Le, "Learning Transferable Architectures for Scalable Image Recognition (cvpr)," in *2018 IEEE Conference on Computer Vision and Pattern Recognition (CVPR)*, Salt Lake City, USA, Jun. 2018, pp. 8697–8710.
- [17] S. Kim and J. Browne, "A general approach to mapping of parallel computation upon multiprocessor architectures," in *Proceedings of the International Conference on Parallel Processing*, Pennsylvania State University, PA, USA, Aug. 1988, pp. 1–8.
- [18] ONNX runtime. [Online]. Available: <https://github.com/microsoft/onnxruntime>
- [19] B. Kruatrachue and T. Lewis, "Grain size determination for parallel programs," *IEEE Software*, vol. 5, Issue 1, pp. 23–32, Jan. 1988.
- [20] "Pytorch 2.0." [Online]. Available: <https://pytorch.org/get-started/pytorch-2.0/>
- [21] Huggingface - Models. [Online]. Available: <https://huggingface.co/models>
- [22] ONNX - Models. [Online]. Available: <https://github.com/onnx/models>

- [23] Global Interpreter Lock. [Online]. Available: <https://wiki.python.org/moin/GlobalInterpreterLock>
- [24] The OpenMP API specification for parallel programming. [Online]. Available: <https://www.openmp.org/>
- [25] Intel C++ Compiler Developer Guide. [Online]. Available: <https://www.intel.com/content/www/us/en/docs/cpp-compiler/developer-guide-reference/2021-8/openmp-support-libraries.html>